AIAA SciTech Forum
January 3-7, 2022, San Diego, CA & Virtual
AIAA SCITECH 2022 Forum

10.2514/6.2022-0062

A numerical investigation of the Water-Enhanced Turbofan laboratory-scale ground demonstrator

A. Marcellan*, M. Henke† and S. Schuldt‡
German Aerospace Center, Stuttgart, Germany

P. Maas§ and A. Göhler-Stroh ¶
Bauhaus Luftfahrt e.V., Taufkirchen, Germany

This paper presents the results of a numerical investigation of a laboratory-scale Water-Enhanced Turbofan (WET) ground demonstrator. The demonstrator is being set up at the German Aerospace Center (DLR) Institute of Combustion Technology to prove the technological feasibility of the novel WET concept at an early stage of development and to gain vital insights for further development. In a WET, water condensation from exhaust gas cooling is captured, pressurized, vaporized via exhaust gas energy and then fed into the combustion chamber. The complexity of the system requires a better understanding of the effects of steam injection and recovery mechanism, both of which are to be studied experimentally on a demonstration test rig. The development of this test rig is supported by a preliminary analysis of the system behavior under different water load conditions. A 0-D model of the test bench is developed, thereby allowing for the numerical investigation of the test bench and its possible configurations, which would support the development process of its main components. This paper presents the test rig, the modelling approach, and the results of the preliminary numerical investigation. The effects of increased pressure drops at the inlet and outlet of the selected gas turbine on critical engine parameters are analyzed, the operation of the bleed valves is investigated, different performance properties for the condenser unit are explored, and, to conclude, the effects of separation channels efficiency in the water recovery unit are examined.

I. Introduction and State of the Art

Pursuing the targets of the Flightpath 2050 program [1], a reduction of 75% in CO_2 and 90% in NO_x emissions, the aviation industry has to look beyond incremental improvements of the Brayton cycle and investigate new engine concepts. Therefore, a consortium of industrial, university, and national research institutions has been established to investigate and demonstrate innovative solutions to outperform conventional aircraft gas turbines [2]. A very promising concept is the Water-Enhanced Turbofan (WET), wherein water is condensed from the exhaust gas, compressed, evaporated via heat from the exhaust gas, and injected into the engine combustion chamber [3]. This novel aircraft propulsion concept for the time-frame beyond 2030 is predicted to enable a mission fuel reduction of >15% [3] compared to conventional engines of the same technology level, i.e. approx. 40% compared to the EIS 2000 [1]. Furthermore, it shows the potential for >80% reduction in NO_x emissions as well as relevant condensation trail reduction. The concept is advantageously operable with sustainable fuels and hydrogen. In addition, it is scalable for any mission profile and at the same time compatible with fan and open rotor. By increasing the specific power [4] [5], it is also conducive to hybrid-electric propulsion concepts.

Variations of the humidified gas turbine cycle have been studied by several groups around the world since the early 20th century. The work of Jonsson and Yan [4] provides a comprehensive review of the literature on the research and development of humidified gas turbines. The first steam injection for both power enhancement and NO_x control started in the 1970s: Rolls-Royce and Westinghouse began working on steam-injected combustors [4], General Electric (GE) patented a steam-injected gas turbine [6], and Golod et al [4] reported experimental studies of steam injection in a

*Researcher, Institute of Combustion Technology, Pfaffenwaldring 38-40, 70569 Stuttgart, Germany.
†Group Leader, Institute of Combustion Technology, Pfaffenwaldring 38-40, 70569 Stuttgart, Germany.
‡Researcher, Institute of Combustion Technology, Pfaffenwaldring 38-40, 70569 Stuttgart, Germany.
§Research Associate, Visionary Aircraft Concepts – Research Focus Area Energy Technologies and Power Systems, Willy-Messerschmitt-Str. 1, 82024 Taufkirchen, Germany.
¶Dr., Visionary Aircraft Concepts – Research Focus Area Energy Technologies and Power Systems, Willy-Messerschmitt-Str. 1, 82024 Taufkirchen, Germany.

two-shaft gas turbine. After the first Cheng cycle patents [7], several commercial steam-injected gas turbines were developed. Steam-injected gas turbines became more common in the mid-1980s, and several hundred are in operation today. The first commercial Cheng gas turbine was the 501-KH5, based on Rolls-Royce's single-shaft aeroderivative Allison 501-KB gas turbine, which began operation in 1985 at a university in California, generating electricity and steam for space heating and cooling. The Kawasaki M1A-13 gas turbine was also converted to a Cheng version, the M1A-13CC, and the first unit was commissioned in Japan in 1988 [4]. Since then, over one hundred Cheng cycles have been installed [8]. Operating experience with Cheng cycles comes from Kellerer and Spangenberg [9], who describe a 501-KH5 Cheng cycle for cogeneration and district heating that was commissioned at a German university in 1996. Penning and de Lange [10] described two 501-KH5 Cheng cycles for cogeneration in a cardboard factory in operation since 1993. Macchi and Poggio [11] described the first 501-KH5 Cheng cycle with water recovery installed in an Italian car factory. GE offers steam injection systems (STIG) to improve the performance of its aeroderivative gas turbines. The Ukrainian company Zorya-Mashproekt offers the Aquarius system, a gas turbine with steam injection and water recovery. The system is designed for power generation and mechanical propulsion. In November 2003, the first commercial "Aquarius-16" unit with 16 MW capacity was commissioned for a gas pipeline [12].

Today, it has been demonstrated in several power plants that gas turbines can be operated with a humidified working fluid and that the water can be recovered from the exhaust gas and reused in the cycle [4]. Aircraft derived gas turbines appear to be more suitable for operation in humidified cycles than industrial gas turbines because the compressor has a larger surge margin, which allows injection of the steam generated from the exhaust gas without stalling the compressor. To date, however, water injection in aircraft engines has been used only to increase thrust during takeoff [13], and no closed-loop water system has yet been implemented. Many technical issues remain to be resolved, and knowledge transfer and cooperation between academia and industry could be helpful in solving the challenges. In close connection with the European Clean Aviation Programme, the cooperative project DINA2030+ aims to demonstrate the WET proof of concept by numerical simulation and test-bench experiments up to a technology readiness level (TRL) of 4 [2]. The long-term goal is to integrate the WET engine into a full-scale aircraft. Since testing novel gas turbine cycles on a turbofan is extremely complex and not suitable for basic experiments, the demonstration of the WET concept was developed as a step-by-step process, as shown in Fig.1.

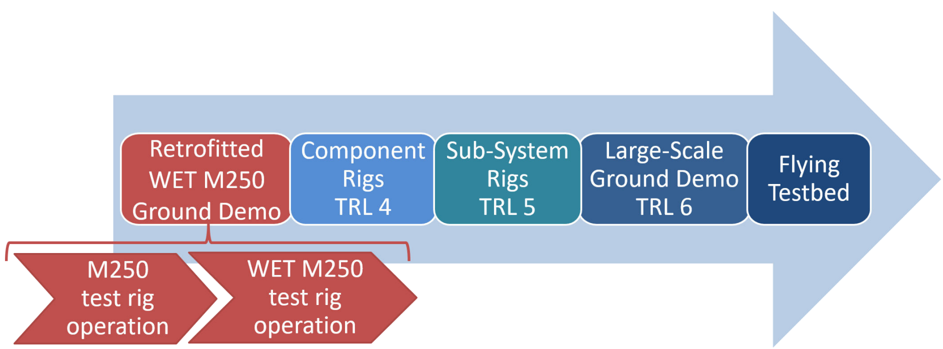

Fig. 1 WET Concept Demonstration strategy.

The turbofan is to be eventually operated in large-scale test rigs at MTU Aero Engines; to this aim, models of the components physics and behavior must first be created and validated, which require a simpler setup. At the DLR Institute of Combustion Technology, a laboratory-scale test rig, based on a Rolls Royce M250 C20B series turboshaft engine, is currently in development. This rig has been equipped with detailed instrumentation and a generator to emulate different load scenarios.For this demonstration test rig, the M250 engine has been chosen over other conventional aviation turboshaft engines, specifically due to its special architecture. The external combustion chamber is easily accessible and replaceable, and the air from the compressor is guided to the combustor via two external tubes, thereby allowing for the decoupling of the mass flows downstream of the compressor and for the re-feeding of external mass flows into the combustion chamber. These features are useful for the planned cycle demonstration. The test rig will be extended with the custom made steam-related components: the in-house developed combustor with the steam injection system and the components for water recovery. These components will be integrated into the engine, the system will be instrumented in detail, and then measured in operation.

The major goals of the ground demonstration are the evaluation of the technical feasibility, the identification of further needs for component development, and the delivery of validation data and correlations for the numerical tools.

The findings will be incorporated into the models of the project partners Bauhaus Luftfahrt e.V. (BHL) and MTU in order to design the target systems and the large-scale demonstrator. With this aim, the M250 test rig gas turbine, as well as the projected modifications, have been analyzed numerically beforehand in order to allow for the design, construction, and operation of required hardware, test rig infrastructure, and instrumentation. Both DLR, focusing on the laboratory-scale ground test stand, and BHL/MTU, concentrating on the target systems, benefit from the know-how that can be provided by the approach presented here.

The laboratory-scale test rig at the DLR Institute of Combustion Technology is presented in Section II. The rig has been modeled with the in-house developed Micro Gas Turbine Steady-State Simulator (MGTS^3) tool, which is presented in Section III. The M250 turboshaft is first modeled and verified with data from the available literature (Subsection III.A). Then, the WET-specific components like steam generator, condenser, liquid water recovery system are implemented, as presented in Subsection III.B. Both full-load and part-load behavior are accounted for, as well as for phase change of the fluid. Modification and extension of the ideal gas model are conducted in order to account for higher water-gas-ratios as well as the phase changes. A key challenge for the test rig is to connect the novel concept components to the M250 gas turbine flow path and to achieve and maintain a stable gas turbine operation. To this end, a bleed valve is to be integrated at the compressor outlet to discharge the compressor and stabilize the turbo components when a large amount of steam is injected (water-balancing bleed valve). In the first study in Section IV, the effects of increased pressure drops at the inlet and outlet of the M250 gas turbine due to necessary laboratory infrastructure, instrumentation, and WET components on critical engine parameters are analyzed. In Section V, the results of the analysis of the test rig with WET components is presented. Here, the behavior of the water-balancing bleed valve is investigated, allowing a better understanding of the effects of varying water content on the turbo maps and on the main engine parameters, such as turbine outlet temperature. A preliminary design investigation of the condenser unit is performed, varying the minimum pinch to optimize the amount of condensed water in the exhaust gas. Finally, the effect of separation channels efficiency in the water recovery unit (WRU) on the achievable amount of condensed and recovered water is also investigated.

II. Laboratory-scale ground demonstrator

The WET concept will be demonstrated in a test rig designed for this purpose, which is being developed at the DLR Institute of Combustion Technology in Stuttgart. The first step is to test the gas turbine test bench based on the RR M250 C20B gas turbine without cycle modifications. The aim is to characterize the baseline system, the connected laboratory infrastructure, and its influence on the machine. The M250 C20B gas turbine is a two-spool turboshaft engine for small helicopters. A three-quarter section of the engine is shown in Fig.3a. The engine has a compressor with six axial stages and a centrifugal output stage. A bleed valve after the fifth axial stages ensures the stability of the compressor in part-load operation. The pressure housing directs the flow by 180 degree to the axial can combustor. Housing and combustor are located outside the rotating parts, making it easily accessible for the necessary cycle modifications. The two-stage axial high-pressure turbine drives the compressor. The downstream low-pressure turbine also has two axial stages and delivers the mechanical power to the transmission gear and output shaft.

In Fig.2 the M250 is shown in the laboratory together with the integrated generator/inverter. The high-power-density generator with integrated inverter is mounted in front of the gearbox below the compressor and connected to the output shaft of the power turbine. The gear ratio of the transmission was modified to increase the output rotational speed from 6000 rpm to 14280 rpm due to the high speeds required by the generator. The electric machine converts the shaft power into DC current, which is fed into the grid via a DC link and additional DC/AC inverter units. The combination of gas turbine and generator/inverter is called GenSet: it achieves a power density of 2.65 kW/kg with an output of 310 kW and it is also used for hybrid electrical propulsion in further research projects. The rig is planned to be instrumented in detail with temperature, pressure, mass flow and rotational speed sensors at all relevant positions. Also under development is a FADEC (Full Authority Digital Engine Control) to control the machine with the in-house designed staged FLOX combustor for high water contents.

For the demonstration of the WET concept, the baseline gas turbine test rig will be extended to include a number of steam-related components. The closed water cycle of the WET concept [3] is characterized by a heat exchange between the hot humid exhaust gas and the water that is evaporated before injection into the combustion chamber. In the test rig this exchange is replaced by an open water cycle. Here, an evaporator is used to boil and heat the water vapor, while two heat exchangers are integrated downstream of the power turbine, to emulate the functionalities of the WET condenser. The first heat exchanger is used to cool the hot humid exhaust gas, while the second heat exchanger, called the condenser, with a different coolant, is set up to achieve condensation of the water vapor. This allows more flexibility for the experimental investigation. A schematic of the planned implementation is shown in Fig.3b.

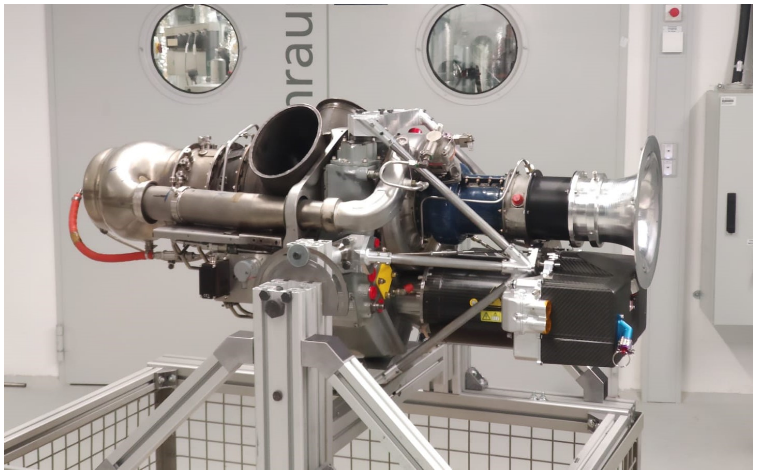

Fig. 2 M250-based GenSet in the DLR laboratory.

First, water is pumped into the evaporator where it is boiled and heated to the desired temperature. The super-heated steam is then injected into the combustion chamber (station 3 in Fig.3b). To avoid unstable behavior of the original M250 turbo components, part of the air is discharged after the compressor via an additional bleed valve (water-balancing bleed), compensating for the additional steam mass flow in the cycle. The hot exhaust gas with high water content provides power to the high-pressure and low-pressure turbines. After exiting the power turbine (station 5), the hot and humid gas flow is split into two parts: most of the flow leaves the system through the exhaust chimney (station 8a), whereas a small part of the hot gas is used to test the developed technologies for water recovery. This is done in order to keep all WET-components more compact and thus enable easier manageability on a laboratory scale. First, the hot and humid exhaust gas is cooled in a heat exchanger. Then a condenser is integrated, which provides sufficient cooling to condense a major part of the vapor. The exhaust gas with water droplets then enters the water recovery unit where the liquid water is separated from the gas and measured. The cold and saturated exhaust gas finally exits the system in station 8b.

The aim of the investigations with this test rig is to understand the behavior and interrelationships of the components as far as possible, to highlight the main challenges of the concept, and to demonstrate its functionality in principle.

III. Numerical model

The test rig is modeled in the in-house developed tool MGTS^3 implemented with Matlab®/Simulink®. The tool is used for fast and robust 0-D steady-state simulations of complex MGT-based cycles. It allows for the variation of complex system parameters for design point studies and investigation of off-design characteristics. Gas flows are modeled as ideal gas mixture, where heat capacity, viscosity, and heat conductivity of the pure substances are calculated with temperature dependent polynomials. The composition of the gas after the combustion chamber is calculated with the assumption of complete combustion. More details about the simulator are discussed in [15] and [16].

In the first step, the M250 gas turbine was modeled in cooperation between DLR and BHL. While no experimental data is yet available for the actual M250, the models from DLR and BHL were validated and compared using data from the literature [17]. For the M250 gas turbine, the WET configuration results in a marked increase in complexity. For the targeted larger aircraft engines, the increase in complexity due to this configuration is even more significant. Therefore, modeling these systems without validation data from a test bench can lead to incorrect assumptions and simplified models that miss phenomena that are not known at this stage of development. These risks will be mitigated by validating the models based on test data from the retrofitted WET M250 ground demonstrator. In this step, model inaccuracies or significant effects that were previously neglected are expected to become visible, leading to the necessary model improvements. While DLR is focusing on the retrofitted WET M250 ground demonstrator and associated process modeling, the primary goal is to improve BHL and MTU's design process for the target WET engines. Therefore, BHL and DLR consider the congruence of their modeling approaches to be fundamental for transferring the knowledge gained during model validation to the full-scale BHL and MTU design process.

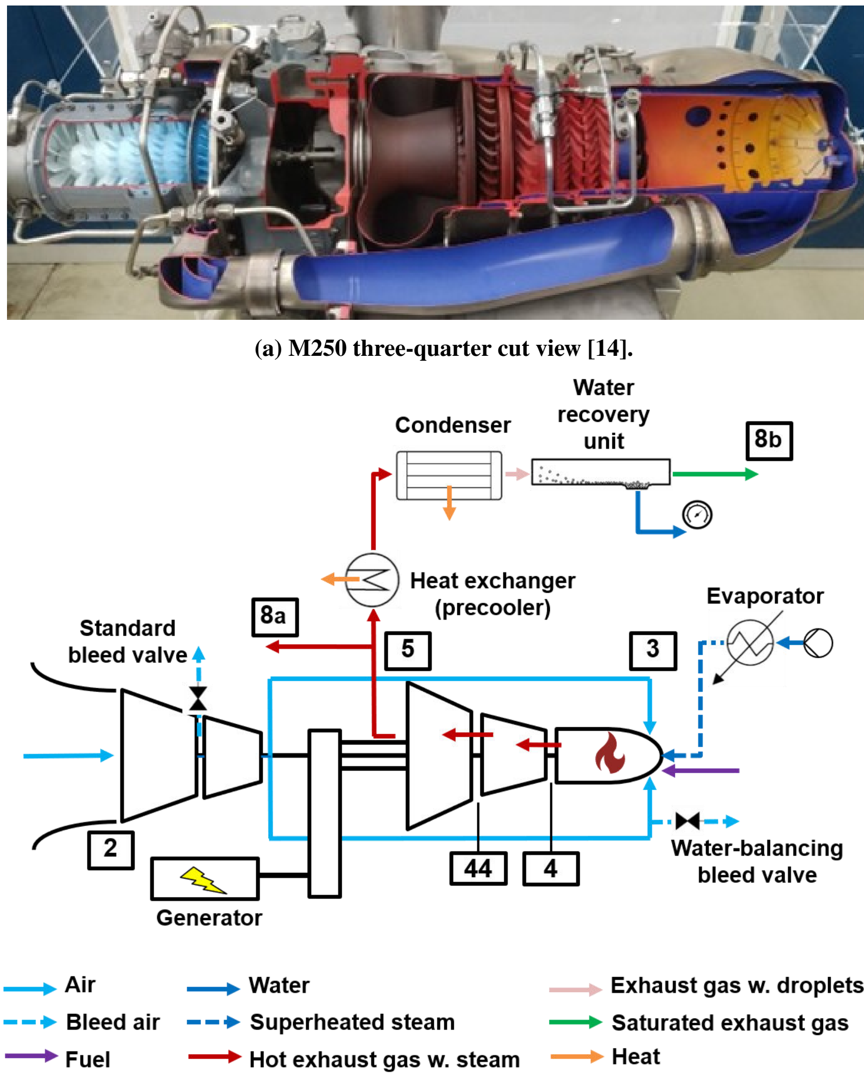

Fig. 3 Test rig layout and gas turbine view.

A. RR M250 C20B gas turbine model

DLR and BHL models for the M250 gas turbine are implemented in two different simulation frameworks for different sizing tasks (test rig environment vs. engine preliminary design). In order to align and compare the modeling approaches, common literature sources and performance sheets [17] [18] were used as boundary and validation data containing all performance parameters such as design shaft power, design speed, and design turbine exit temperature, amongst others. Model and component assumptions such as design parameters, components efficiencies, duct pressure losses, and handling bleeds have been checked for commonality. The resulting model agreement was verified by comparing thermodynamic properties in all relevant operational conditions. The part-load characteristics for the machine inlet and nozzle pressure losses, burner efficiency, and handling bleeds behavior (standard bleeds for compressor axial stages stability and turbine cooling) based on available data from literature [17] have been integrated in the engine model using non-linear regression for off-design analysis.

The performance of turbomachinery is calculated through interpolation from user specified maps according to the actual operating point. The turbo component maps have been matched, first by selection of the appropriate common maps, then by matching the map interpolation and scaling methods. For the axial-radial compressor of the M250 the map has been obtained from the PhD thesis of Menrath [18]. For the high work low aspect ratio turbine of the gas generator, the map of the NASA-TM-83655 in the GasTurb Map Collection3 has been selected. The low-pressure turbine map of the M250 has been digitalized from data available in [18]. All maps have been first adjusted according to the Reynolds correction factors based on temperature, pressure, and viscosity, as defined in GasTurb efficiency and mass flow correction method [19]. Afterwards, standard scaling factors on mass flow, pressure ratio, and efficiency have been obtained from design calculation in order to match the literature data in Maas [17]. To compare the turbo maps, a number of different inlet conditions (temperature and pressure) were tested at different speeds and pressure ratios. For each combination of inlet data, the mass flow rate and efficiency of the turbo components were calculated. Figure 4 shows the results of a selection of the inlet data tested for the compressor with mean and maximum deviation for the mass flow and efficiency calculations. The table beside summarizes the results for all calculated parameters of the turbo maps.

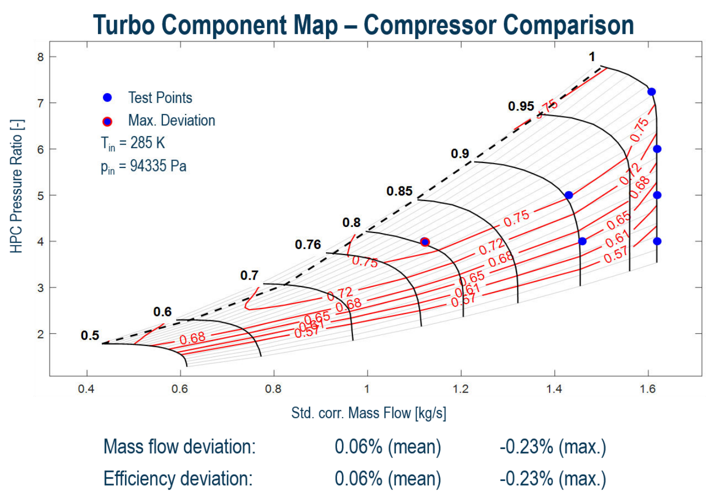

	Compressor		High pressure turbine		Low pressure turbine	
	mean	max	mean	max	mean	max
Mass flow deviation	0,06%	-0,23%	0,02%	0,07%	0,01%	0,01%
Efficiency deviation	0,06%	-0,23%	0,02%	0,07%	0,01%	0,02%

Fig. 4 Turbomaps comparison between DLR and BHL.

Figure 5 shows the operating line with simulated points and reference data on the compressor map. Good agreement was obtained between the two models with an absolute deviation of all relevant parameters below 0.53%. When comparing the results of the two models with the reference data in Mass [17], a maximum deviation of 2.91% for the DLR model and 2.89% for the BHL model at 52% design shaft power were found. These differences are attributed to the uncertainty of the inlet conditions of the high-pressure turbine, since the reference values for T4 in Mass [17] were not directly measured but back-calculated and, for example, cooling influences were not taken into account.

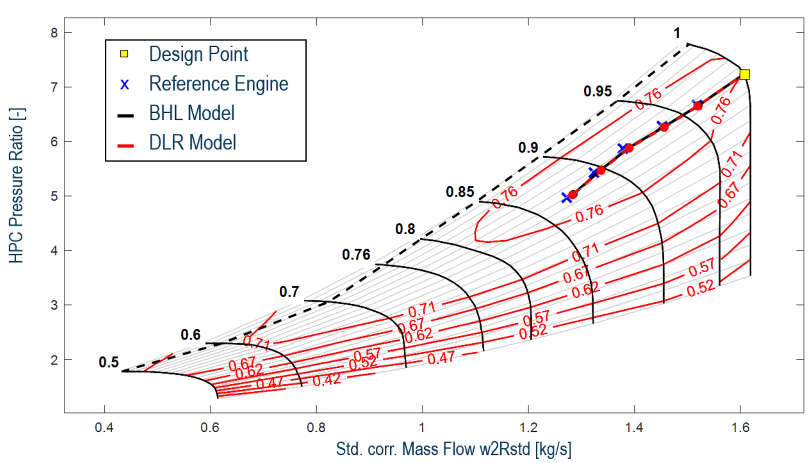

Fig. 5 Operating line on compressor map with modeled data points and reference values.

Due to engine-to-engine variation, measurement data from an acceptance run for the actual M250 gas turbine purchased for the test rig was used to adjust the map scaling factors at full load. The model was run at all power settings for which measured data were also available, and the calculated performance showed good agreement with the measurements.

B. WET component models

The WET components modeled in the tool were the evaporator, the heat exchanger after the power turbine, the condenser, and the water recovery unit (WRU). For the evaporator, a black-box approach for the modeling was chosen, since the particular operation of the component is not of interest for the scope of the investigation. The main input parameters are the desired outlet temperature and pressure of the water vapor, which can be varied for the numerical investigation.

The heat exchanger for the pre-cooling of the humid exhaust was modeled with a pinch-point approach. For design purposes, this approach allows the identification of the required pinch, i.e. the minimum temperature difference between the hot flow and the cold flow, and its position. Among the physically possible pinch points (water side inlet, hot gas side inlet) the heat exchanger/precooler model allows the solver of the system to find the best design pinch, with the condition of still having liquid water exiting the cooling side of the component, while almost reaching the dew point at the gas side outlet. Pressure losses on both sides can be given as a relative value compared to the inlet pressure. As mentioned above, the heat transfer from the exhaust gas to the evaporator and to the environment is not part of the investigation. Therefore, the test rig will feature an industrial water/gas heat exchanger, which has a much lower pressure drop. This allows for a wider range of possible WRU pressure losses downstream and thus gives the test rig more flexibility. A relative pressure loss of 1% was assumed for this component.

The development of the condenser unit and the WRU is a task undertaken by the Institute of Aerospace Thermodynamics (ITLR) at the University of Stuttgart. At this preliminary stage of the project, results from the generic experiments planned to investigate different methods of water recovery by ITLR are not yet available. Therefore, the architecture of the components to be integrated in the test rig are still unknown and preliminary investigation on the effects of design parameters was performed. With this aim, the condenser unit was modeled with a pinch-point approach where design pinch, pressure losses, and limiting condition from the cooling water side can be investigated. Since no geometries are required for the model, only design point studies were performed. Figure 6 shows schematically the pinch point concept. The x-axis shows the heat transferred, while the y-axis indicates the temperatures of the two media. Both the precooler and condenser are shown in one image, with the transition point highlighted. Two different cooling circuits are used for the two components: the on-site water heating circuit for the precooler and the water cooling circuit, at much lower working temperatures, for the condenser. The WRU was modeled at this stage using a black-box approach, with the main design parameters being the efficiency of the separation channels and the pressure drop. The efficiency of the separation channels is defined as the ratio of fully recovered water to condensed water entering the component in the exhaust gas.

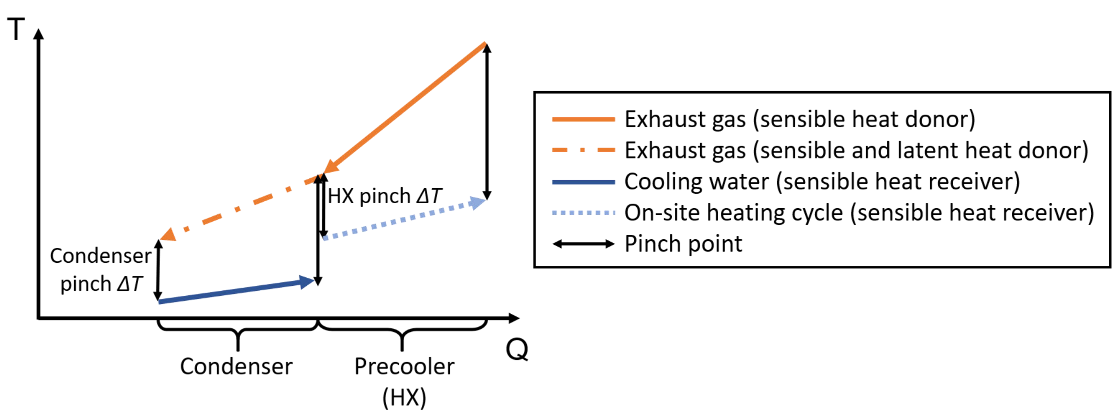

Fig. 6 Pinch points diagram for the heat exchanger and for the condenser.

IV. Study I: Analysis of the RR M250 C20B test rig without cycle modifications

Here the results of simulations of the test rig with the M250 engine under full load and part load are presented.

A. Standard bleed valve behavior

The effects of opening/closing of the standard bleed valve used for ensuring the stability of the axial stages of the compressor are here presented. In Fig.7 the behavior of the bleed valve, which is based on data from the available literature, is shown on the compressor map. When starting the machine, the standard bleed valve is in open position. During the ramp-up procedure, depending on the ambient temperature and rotational speed, the standard bleed valve is closed. The resulting compressor discharge pressure is depicted in 8a. A significant pressure rise in the system after the closing of the standard bleed valve is visible. The air and fuel mass flows entering the combustion chamber are pictured in 8b for the machine operating range. The air mass flow increases considerably when the bleed valve is closed, so that the turbine can deliver more power and less fuel is needed to reach the set power of the machine.

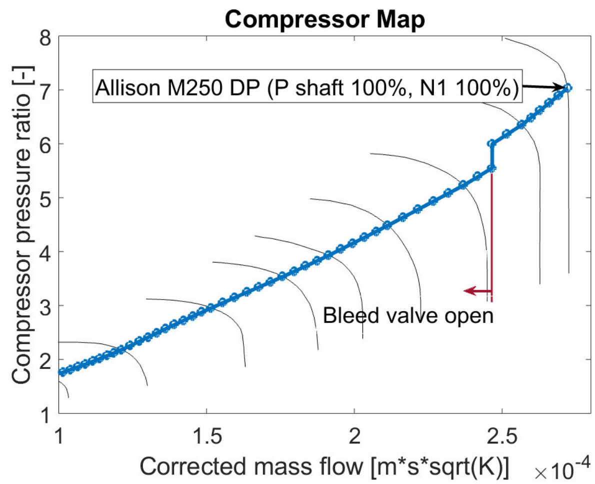

Fig. 7 Effects of opening/closing of the bleed valve on the compressor operating line.

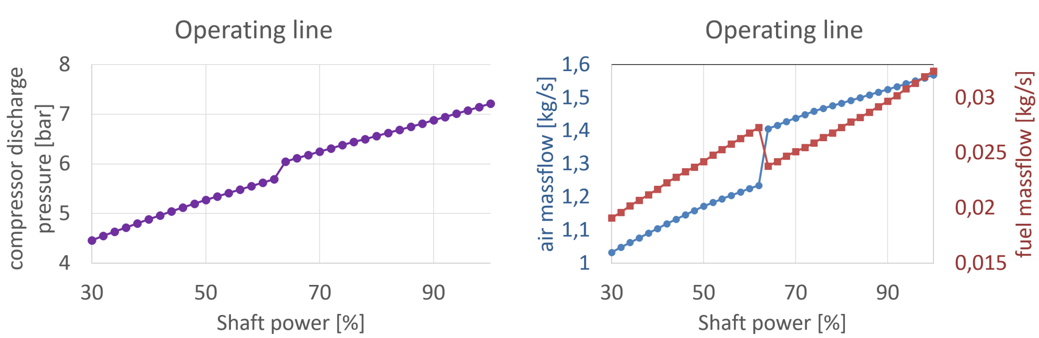

(a) Effects on compressor discharge pressure. **(b) Effects on air and fuel flow entering the burner.**

Fig. 8 Standard bleed valve behavior.

In Fig.9 the lambda in the combustion chamber is shown. Lambda represents the ratio between the actual air-fuel ratio and the stoichiometric air-fuel ratio. Depending on the value of lambda, the engine operates in the lean ($\lambda > 1$), stoichiometric ($\lambda = 1$) or rich ($\lambda < 1$) air-fuel mixture regime. The lambda value rises when the valve is closed due to the increase in the air flow entering the combustion chamber and falls again when the system is in full load. As a result, the critical temperatures at the inlet of the high- and low-pressure turbines also drop when the bleed valve is closed, showing a step-like behavior in the simulations.

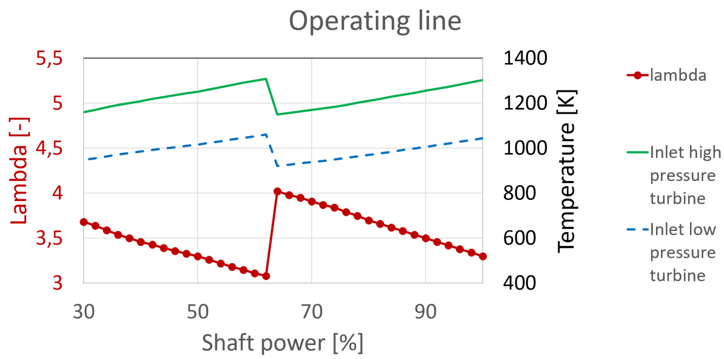

Fig. 9 Behavior of lambda and turbines inlet temperatures.

B. Pressure losses at the engine inlet and outlet

Here, the pressure losses upstream of the compressor and downstream of the power turbine are investigated. The additional pressure losses at the engine inlet are due to the air supply ducts and the stilling chamber, which is implemented directly upstream of the compressor to ensure smooth inlet conditions. The pressure loss after the power turbine represents the pressure losses caused by the exhaust ducts installed in the laboratory and later by the WET components that are integrated into the system. Although the pressure losses affects many process parameters, the most critical influence is on the high-pressure turbine outlet temperature Tt44, which thus limits the tolerable pressure drop. In Fig.10, a variation of the expected pressure losses for 100% shaft power is simulated and the effects on the critical system temperature Tt44 are shown.

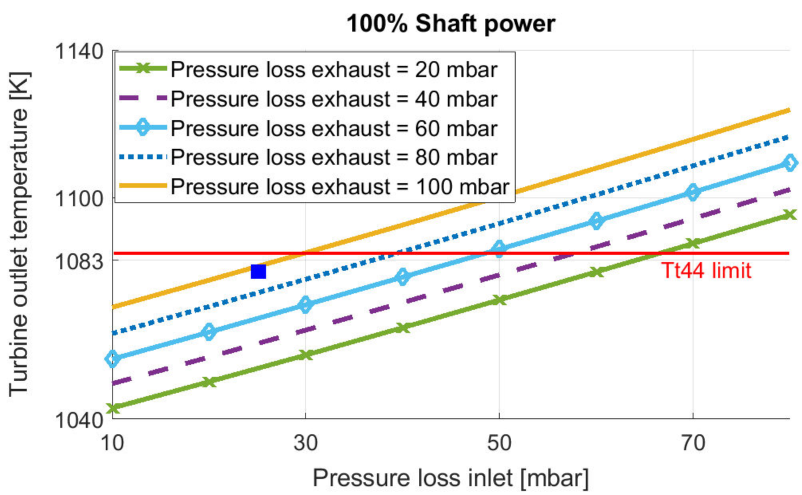

Fig. 10 Impact of pressure losses on Tt44 at full load.

In the diagram, the possible combinations of pressure losses that are not critical for the system are those below the limit line for Tt44. On this basis, the optimized design of the settling chamber at the compressor inlet was developed. For the chamber, CFD calculations showed an absolute pressure drop of 10 mbar at design point (to take into account the additional losses in the air supply ducts). An overall pressure drop upstream of the compressor of 25 mbar and a pressure loss downstream of the power turbine of 90 mbar were assumed for the following simulations (blue box in the figure).

V. Study II: Preliminary analysis of the WET-M250 test rig

The main design parameters of the M250 engine test rig with WET components have been investigated and the results are presented in the following sections.

A. Water-gas ratio and bleed-water ratio variations

One of the most important design parameters of the WET test rig is the water-gas ratio (WGR). The WGR is defined as the amount of water present at the burner inlet in relation to the total gas entering the burner, i.e. the air from the compressor (without taps) and the superheated steam.

When steam is injected into the M250 cycle, the turbomachine equilibrium is destabilized as the matching between compressor and turbine is no longer guaranteed. To avoid damage to the WET-M250 test rig, a portion of the pressurized air is therefore blown off after the compressor via the additional water-balancing bleed valve. The amount of bleed air mass flow in relation to the amount of water mass flow injected is defined as the bleed-water ratio.

The WGR and the bleed-water ratio have been varied to better understand their effects on turbomachinery performance. Figure 11 shows the compressor map with a blue line indicating the original operating line of the M250. A blue dot shows the simulated power setting for the M250 model without WET modifications, and the red dots show the same set shaft power for the WET configuration with different WGR values and bleed-water ratios.

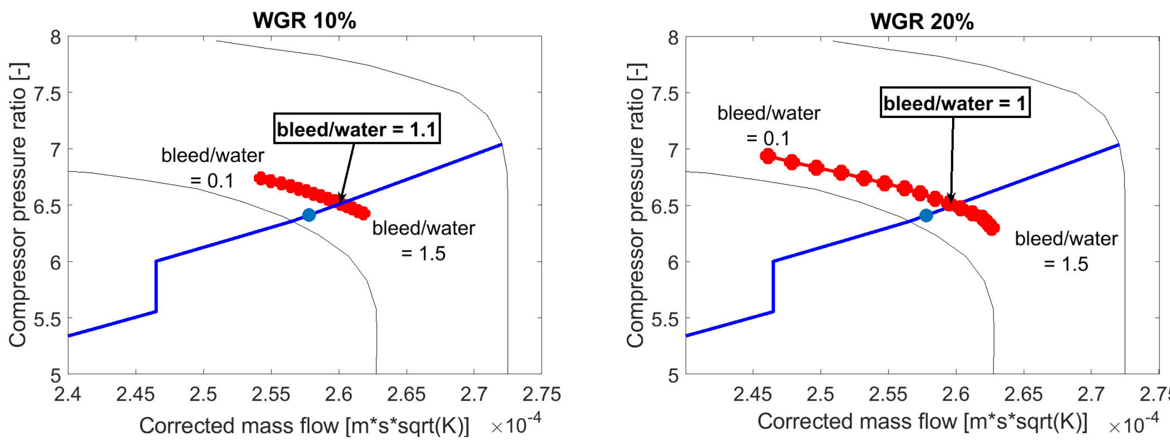

Fig. 11 Variation of additional bleed flow on the compressor map for the WET-M250 test rig at full load.

For each WGR, the air mass flow tapped from the additional water-balancing bleed valve is varied while keeping the target power of the system constant. If more water mass flow is injected into the system than air mass flow is tapped (bleed-water ratio < 1), the operating point of the compressor moves towards the surge line. The ideal value of the bleed-water ratio to ensure optimal turbomachinery performance of the WET-M250 test rig is the one that allows the compressor to operate on the original operating line. This value of the bleed-water ratio is between 1.1 and 1 for the WGRs investigated at full load. For the simulations that follow, it is assumed that the mass air flow tapped from the additional water-balancing bleed valve is set so that the system's compressor still operates on the same operating line as it would in the M250 without water injection.

B. Condenser

Downstream of the power turbine, part of the humid exhaust gases is passed through a heat exchanger in which cooling water provides sufficient cooling capacity to cool the exhaust gases until they reach the dew point before condensation occurs. At this point, a second heat exchanger, called a condenser, transfers additional heat from the exhaust gas to a lower-temperature cooling water circuit that allows condensation of water vapor in the cold exhaust gas. The most important modelling parameter for the condenser is the pinch point. A pinch point is a point in the condenser where the temperature difference between hot and cold fluid is the smallest. Although technically any value greater than zero can provide heat transfer, very small values of these temperature differences are often impractical because they require increasingly larger heat transfer surfaces, i.e. larger heat exchangers.

In Fig.12 the variation of condenser design pinch is investigated for different water to gas ratios. Figure 12a shows the ratio of condensed water to the water injected into the cycle. The diagram shows that a surplus of condensed water in comparison to injected water could be achieved in this particular system with a condenser pinch below 20 K. However, proving the feasibility of a closed water cycle is not the goal of the ground demonstrator. For the high-altitude target system, the conditions and design of the WET engine will be different, and the air temperature will be lower so that more water can be condensed despite the lower air pressure.

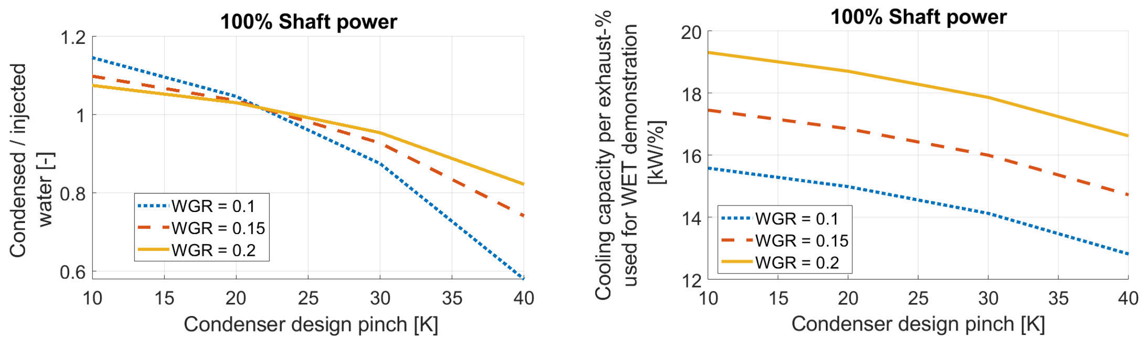

(a) Effects on condensation mass flow. **(b) Effects on required cooling power.**

Fig. 12 Condenser design pinch variations for different water to gas ratio (WGR).

In addition, Fig.12b shows the amount of heat transfer required to first cool the exhaust gases and then condense the water vapor. The cooling power is given per % of exhaust mass flow, because only a fraction of the exhaust gas flow will be fed into the heat exchanger and condenser as described in section II. For example, the diagram shows that for 1 % of the exhaust mass flow used for the WET demonstration, 18.7 kW of cooling power is required for a WGR of 0.2 and a condenser with a 20 K design pinch. This information is used to determine the desired proportion of exhaust gases to be redirected through the WET components.

C. Water recovery unit

The condensed water droplets gained after the heat exchanger and the condenser needs to be recovered for demonstrating the WET concept. This is done in the WRU, which is a critical component developed by the project partner ITLR. The efficiency of the separation channels in this component is investigated in Fig.13. Here a pinch of 15 K is assumed for the condenser. Similar as for the condenser analysis, the graph shows the ratio of water recovered to water injected into the circuit. The graph shows that in this particular system, a separation channel efficiency of over 89% at a WGR of 0.1, over 92% at a WGR of 0.15, and over 94% at a WGR of 0.2 would result in a surplus of recovered water.

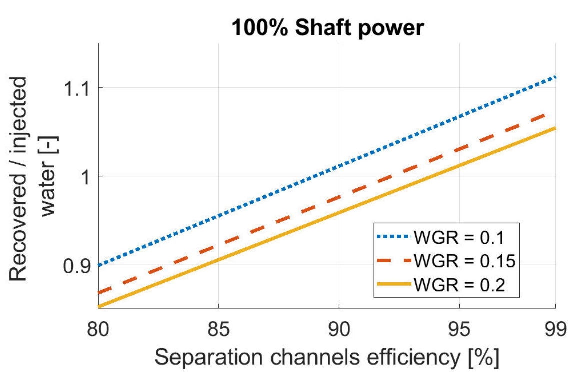

Fig. 13 Effects of separation channels efficiency for different WGR.

VI. Conclusion

To investigate the technological feasibility of a novel WET concept, a laboratory-scale ground demonstrator was mathematically modeled. The numerical results helped drawing fundamental considerations for the development of the test rig with the unmodified M250, e.g. with regard to possible pressure losses. The impact of the standard bleed valve on operation behavior was investigated and it was shown that the operation of the valve also affects process critical temperatures. From the pressure drop analysis at the gas turbine inlet and gas turbine outlet, relevant values for the maximum permissible pressure drop due to the laboratory infrastructure, measurement instrumentation and

WET components were determined. On this basis, the optimized design of the settling chamber at the compressor inlet was developed with an absolute pressure drop at the design point of 10 mbar. From the analysis of the turbine outlet temperature increase due to the additional pressure losses in the flue gas ducts, a maximum pressure drop of 90 mbar was determined for the selection of the WET components and the exhaust duct design. If this pressure drop is exceeded, measures should be taken to prevent over-temperature operation of the system.

In addition, the simulations showed that the test rig is well suited to demonstrate WET operation and provided useful information for the development of the final test rig: understanding the response of the compressor once water is introduced into the cycle enables the required bleed mass flow of the water-balancing bleed valve to be determined for safe operation of the test rig. This is needed for the development of the control system of the WET test rig. The preliminary analysis for the condenser unit was used to determine the influence of the component pinch point on the achievable condensation for various water-gas ratios. The required cooling capacity per % of exhaust mass flow diverted through the WET components was determined, e.g., to set upper limits for the condenser exhaust mass flow, according to the laboratory cooling capacity, to be used in the design of the WET test rig.

In the future steps, the test bench model will be validated with measurement data from the M250 test rig. This will improve the model prediction of the system behavior and help the further development of the WET-M250 test rig. These process and modelling insights, together with experimental data from additional component test benches, will enable the design of large-scale test rigs at MTU and ultimately the design of commercial WET-engines.

Acknowledgments

The authors like to thank MTU Aero Engines for the permission to publish this paper. The research work of MTU Aero Engines and DLR associated with this publication has been supported by the German Federal Ministry for Economic Affairs and Energy under grant number 20T1720. The funding of the work through the 3rd call of the Federal Aviation Research Program V (LuFo V-3), grant project title "VerVal", is gratefully acknowledged. The authors are responsible for the content of this publication.

References

[1] Flightpath, A., "2050-europe's vision for aviation," *Advisory Council for Aeronautics Research in Europe*, 2011.

[2] Schmitz, O., Kaiser, S., Klingels, H., Kufner, P., Obermüller, M., Henke, M., Zanger, J., Grimm, F., Schuldt, S., Marcellan, A., et al., "Aero Engine Concepts Beyond 2030: Part 3—Experimental Demonstration of Technological Feasibility," *Journal of Engineering for Gas Turbines and Power*, Vol. 143, No. 2, 2021, p. 021003.

[3] Schmitz, O., Klingels, H., and Kufner, P., "Aero Engine Concepts Beyond 2030: Part 1—The Steam Injecting and Recovering Aero Engine," *Journal of Engineering for Gas Turbines and Power*, Vol. 143, No. 2, 2021, p. 021001.

[4] Jonsson, M., and Yan, J., "Humidified gas turbines—a review of proposed and implemented cycles," *Energy*, Vol. 30, No. 7, 2005, pp. 1013–1078.

[5] Kolp, D., and Moeller, D., "World's First Full STIG™ LM5000 Installed at Simpson Paper Company," *Journal of Engineering for Gas Turbines and Power*, 1989.

[6] Kydd, P. H., and Day, W. H., "Steam Injection in gas turbines having fixed geometry components," , Sep. 26 1972. US Patent 3,693,347.

[7] Cheng, D. Y., "Regenerative parallel compound dual-fluid heat engine," , Dec. 12 1978. US Patent 4,128,994.

[8] Cheng, D. Y., and Nelson, A. L., "The chronological development of the Cheng cycle steam injected gas turbine during the past 25 years," *Turbo Expo: Power for Land, Sea, and Air*, Vol. 3607, 2002, pp. 421–428.

[9] Kellerer, A., and Spangenberg, C., "Operating Experience with a Cheng Cycle Unit Concept and Technical Characteristics," *VGB PowerTech*, Vol. 11, 1998, pp. 16–22.

[10] Penning, F., and De Lange, H., "Steam injection: analysis of a typical application," *Applied Thermal Engineering*, Vol. 16, No. 2, 1996, pp. 115–125.

[11] Macchi, E., and Poggio, A., "A cogeneration plant based on a steam injection gas turbine with recovery of the water injected: design criteria and initial operating experience," *Turbo Expo: Power for Land, Sea, and Air*, Vol. 78866, 1994, p. V004T11A002.

[12] Movchan, S. N., Romanov, V. V., Chobenko, V. N., and Shevtsov, A. P., “Contact Steam-and-Gas Turbine Units of the “AQUARIUS” Type: The Present Status and Future Prospects,” *Turbo Expo: Power for Land, Sea, and Air*, Vol. 48852, 2009, pp. 703–709.

[13] Bathie, W. W., *Fundamentals of gas turbines*, John Wiley and Sons, New York, 1996.

[14] Schuldt, S., “M250 three-quarter cut view,” , 28 May 2019. Unpublished photograph taken at the Universität der Bundeswehr München.

[15] Henke, M., Klempp, N., Hohloch, M., Monz, T., and Aigner, M., “Validation of a T100 Micro Gas Turbine Steady-State Simulation Tool,” *Turbo Expo: Power for Land, Sea, and Air*, Vol. 3, 2015, p. 42090.

[16] Krummrein, T., Henke, M., and Kutne, P., “A highly flexible approach on the steady-state analysis of innovative micro gas turbine cycles,” *Journal of Engineering for Gas Turbines and Power*, Vol. 140, No. 12, 2018.

[17] Maas, P., “Entwicklung und Validierung eines Triebwerksmodells mittels MATLAB / Simulink,” Master’s thesis, Lehrstuhl für Turbomaschinen und Flugantriebe, Technische Universität München, München, Germany, 2018.

[18] Menrath, M., “Experimentelle Kennwertermittlung und Systemanalyse bei Hubschrauber-Gasturbinen,” Ph.D. thesis, Lehrstuhl für Flugantriebe, Technische Universität München, München, Germany, 1989.

[19] *GasTurb 13 Manual: Design and Off-Design Performance of Gas Turbines*, GasTurb GmbH, available at https://gasturb.com/Downloads/Manuals/GasTurb13.pdf, (accessed on June 2019), 2018.